Pharmaceutical Research, Vol. 26, No. 8, August 2009 (© 2009)
DOI: 10.1007/s11095-009-9910-6

Research Paper

Semi-Mechanistic Model for Neutropenia after High Dose of Chemotherapy in Breast Cancer Patients

Amelia Ramon-Lopez,[1] Ricardo Nalda-Molina,[1] Belen Valenzuela,[1] and Juan Jose Perez-Ruixo[1,2,3]

Received March 27, 2009; accepted May 10, 2009; published online June 2, 2009

Purpose. To describe the absolute neutrophil counts (ANC) profile in breast cancer patients receiving high-dose of chemotherapy and peripheral blood stem-cells (PBSC) transplantation.
Methods. Data from 41 subjects receiving cyclophosphamide, thiotepa and carboplatin were used to develop the ANC model consisting of a drug-sensitive progenitor cell compartment, linked to the peripheral blood compartment, through three transition compartments. PBSC were incorporated into the first transit compartment following a zero-order process, k_{in}, and the rebound effect was explained by a feedback mechanism. A 'kinetics of drug action' model was used to quantify the HDC effect on the progenitor cells according to a linear function, with a slope (α).
Results. The typical of the ANC at baseline ($Circ_0$), mean transit time (MTT), feedback parameter (γ), k_{in} and α were estimated to be $5{,}610 \cdot 10^6$/L, 3.25 days, 0.145, 0.954 cell/kg/day and 2.50 h/U, respectively. rHuG-CSF shortens the MTT by 92% and increases the mitotic activity by 120%. Bootstrap analysis, visual predictive check and numerical predictive checks evidenced accurate prediction of the ANC nadir, time to ANC nadir and time to grade 4 neutropenia recovery.
Conclusion. The time course of neutropenia following high-dose of chemotherapy and PBSC transplantation was accurately predicted. Higher amount of CD34+ cells in the PBSC transplantation and earlier administration rHuG-CSF were associated with faster haematological recovery.

KEY WORDS: cancer; high-dose chemotherapy; neutropenia; peripheral blood stem cell transplantation; population pharmacokinetics/pharmacodynamics; rHuG-CSF.

INTRODUCTION

High dose chemotherapy (HDC) with the support of peripheral blood stem-cells (PBSC) transplantation has been increasingly used in a variety of cancers (13,16,17,20,34,37,58). Despite the use of standard-dose of adjuvant therapy in breast cancer patients, the prognosis of patients with stage II disease with multiple positive nodes or stage III disease is poor. Actually, 55 to 75% of patients with more than ten positive axillary's nodes will relapse within 5 years and 70 to 90% will do so within 10 years (38,39,47). It has been argued that given the inadequacy of standard-dose of adjuvant chemotherapy in this population and the limited efficacy of HDC in metastatic disease (52), the optimal time for using HDC in breast cancer may be as an adjuvant treatment. However, the clinical evaluation of this strategy have suggested limited effect on the disease free survival and overall survival in high risk breast cancer patients (35,39).

Haematological toxicity is the major cause of treatment-related complications following HDC and PBSC transplantation. It is well known that complications and their severity are directly related to the time to reach short-term haematological recovery (2). The administration of haematopoietic growth factors and PBSC shortly after the HDC resulted in faster haematological reconstitution (3,4,6,11,18,19,48,49,54), and the use of prophylactic antibiotics also diminished the incidence of infectious complications. Taken together, these therapeutic strategies have resulted in a reduction of the morbidity and mortality after HDC and PBSC transplantation in breast cancer patients (1,10,39). Nevertheless, understanding the time course of absolute neutrophils counts (ANC) in patients receiving HDC and quantifying the effect of PBSC and granulocyte colony-stimulating factor (rHuG-CSF) on the haematological reconstitution is of particular clinical value as the vast majority of patients develop severe Grade 4 neutropenia that last more than 5 days.

Pharmacokinetic and pharmacodynamic (PKPD) modelling of neutropenia induced by anticancer agents has been increasing during last years (25,43,53). Semi-mechanistic model have been developed to predict the degree and the duration of the haematological toxicity (14,32). In these models, the system-related parameters account for the physiology of neutrophils with respect to its production and regulation, while the drug-specific parameters quantify the cytotoxic drug effect on bone marrow, providing a better characterization of the underlying mechanism of cytotoxicity and explaining the haematological toxicity observed after different doses and schedules. Initially, the model was successfully applied

[1] Pharmacy and Pharmaceutics Division, Department of Engineering, Miguel Hernandez University, San Juan de Alicante, Alicante, Spain.
[2] C/ Picayo, 3, 46530, Puzol, Valencia, Spain.
[3] To whom correspondence should be addressed. (e-mail: juanjose@amgen.com)

to different drugs such as docetaxel, paclitaxel, etoposide, 2-deoxy-2-methylidenecytidine, irinotecan and vinflunine (14). Later, it was applied to topotecan in adult (30) and pediatric populations (36), indisulam (57), pemetrexed (28,29), diflomotecan (55), ispinesib (26), trabectedin (21) and the combinations epirubicin-docetaxel (46) and fluorouracil-epirrubicin-cyclophosphamide (45). However, this model has not been applied yet to analyze the ANC data following HDC and PBSC transplantation.

In this paper, the semi-mechanistic model proposed by Friberg *et al*. is extended to account for the effect of the PBSC transplantation and haematopoietic growth factors, and is also applied to analyze the time course of ANC from high-risk breast cancer patients receiving HDC with the support of PBSC transplantation and haematopoietic growth factors.

MATERIALS AND METHODS

Eligibility Criteria and Treatments

Forty-one patients with histologically confirmed primary high-risk breast cancer, defined as stage II–III disease with $\geq$10 or $\geq$4 positive axillary nodes after surgery or neo-adjuvant chemotherapy, respectively, or inflammatory breast cancer, were admitted to the Oncology Department at the Clinic University Hospital and Dr. Peset University Hospital of Valencia (Spain), to receive HDC and PBSC transplantation as adjuvant treatment between 1996 y 1999. Staging procedures included complete blood count, renal and liver function tests, chest X-ray, and bone scan. Eligible patients were between the ages of 18 and 65 years old, and each patient had good performance status (ECOG 0 or 1), negative pregnancy test, resting left ventricular ejection fraction was 50% or greater, acceptable bone marrow function (white blood cells > 2,000/μL, granulocyte count > 1,500/μL and platelets > 70,000/μL). Subjects with one or more of the following criteria were not selected: severe renal dysfunction (creatinine clearance < 60 mL/min); liver dysfunction (serum total bilirubin > 2 mg/dL; or ALT and AST > 2.5 times normal upper limit); prior extensive radiation therapy (>25% of bone marrow reserve); prior bone marrow transplantation (BMT) or HDC with BMT or PBSC transplantation support; participation in a clinical trial involving an investigational drug in the past 30 days or concurrent enrolment in another investigational trial; and, any coexisting medical condition that is likely to interfere with study procedures and/or results. A summary of the patient characteristics at baseline is presented in Table I.

Patients received STAMP-V regimen with PBSC transplantation as part of their adjuvant treatment within 6 weeks of surgery and all received induction and stem-cell mobilization chemotherapy with rHuG-CSF three weeks before the start chemotherapy. The STAMP-V regimen (1) consisted of 6 g/m^2 cyclophosphamide, 0.5 g/m^2 thiotepa, and 0.8 g/m^2 carboplatin administered as intravenous infusion over 96 h (Day-7 to Day-4). A 375 mg/m^2 of 2-mercaptoethane sulfonic acid sodium (MESNA) was administered 1 h before the cyclophosphamide infusion began and then, 6 g/m^2 was given as intravenous infusion over 96 h. All patients received prophylactic antiemetic treatment: ondansetron 8 mg t.i.d or tropisetron 5 mg o.d., plus dexamethasone 12 mg b.i.d, during 5 days. Norfloxacin, fluconazol and acyclovir were given as prophylactic oral antibiotics starting the day before HDC (Day-8). PBSC transplantation was infused 3 days after the end of HDC (Day 0). Patients received a daily treatment with

Table I. Summary of Patient Characteristics at Baseline

Subject characteristics	Mean	Standard deviation	Range
Age (years)	47.0	8.6	30–61
Weight (kg)	70	12	45–99
Height (cm)	158	5	149–168
Body surface area (m^2)	1.71	0.14	1.37–2.05
Glucose (g/dL)	107	27	62–207
Urea (mg/dL)	28	6	10–40
Creatinine (mg/dL)	0.8	0.2	0.6–1.0
Bilirubin (mg/dL)	0.4	0.2	0.2–0.8
Uric acid (mg/dL)	4.0	1.3	1.9–6.7
Total proteins (g/dL)	6.9	0.6	5.4–7.9
Alkalyne phosphate (UI/L)	46	12	26–79
AST (UI/L)	10	5	5–23
LDH (UI/L)	139	24	106–202
ALT (UI/L)	16	12	7–56
γ-Glutamyltransferase (UI/L)	17	17	2–66
Hemoglobin (g/dL)	11.7	1.2	7.8–13.5
White blood cells (10^6 cells/L)	5,941	4,075	2,320–20,800
Neutrophils (10^6 cells/L)	4,060	3,735	1,700–17,300
Platelets (10^6 cells/L)	229,000	98,000	73,000–579,000
Duration rHuG-CSF treatment (days),			
Start Day +1 (N=22)	13.5	2.77	10–21
Start Day +5 (N=19)	8.4	2.1	5–14
Amount of CD34+ (cells × 10^{6}Kg)	4.7	2.09	1.3–9.85

ALT, serum alanine aminotransferase; *AST*, serum aspartate aminotransferase; *LDH*, serum lactate dehydrogenase

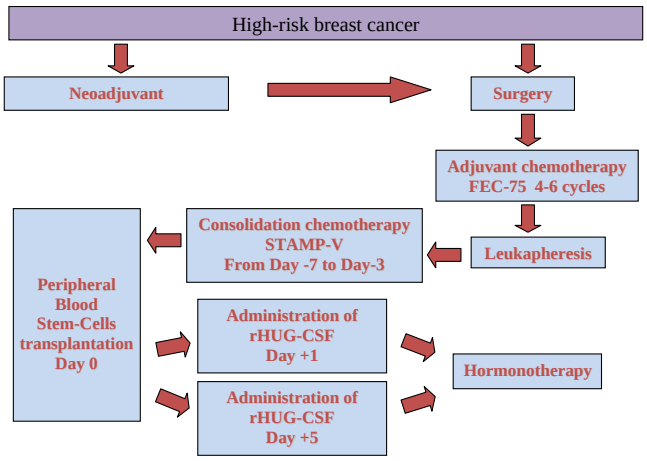

Fig. 1. Schematic of the sequence of treatment.

300 μg of rHuG-CSF and they were randomized to start the rHuG-CSF treatment on Day +1 or Day +5. An schematic figure of the overall therapeutic strategy is displayed in Fig. 1.

The study was conducted following the principles for human experimentation as defined in the Declaration of Helsinki and International Conference of Harmonization, and was approved by the Human Investigational Review Board of each study center. Informed consent was obtained from each subject after being told the potential risks and benefits, as well as the investigational nature of the study.

Blood Sampling Schedule

In each patient, one blood sample was collected before the administration of HDC. Afterwards, daily samples were collected, as part of the routine clinical monitoring, until patient completely recovers from the haematological toxicity. The ANC in blood sample were determined using an automated haematology analyzer (Coulter Counter, Model D industrial, Coulter Electronics, Hialeah, FL, USA).

Model Development

Software

Nonlinear mixed-effects modelling by extended least squares regression using the first-order conditional estimation (FOCE) method implemented in NONMEM V level 1.1 software package (GloboMax, Hanover, MD, USA) (5) was used to develop the pharmacostatistical model and conduct model-based simulations. Compilations were achieved using DIGITAL Visual Fortran Version 6.0A. Graphical and all other statistical analyses were performed using S-Plus 6.1 Professional Edition (Insightful, Seattle, WA, USA).

Pharmacostatistical Model

The semi-mechanistic model proposed by Friberg *et al.* (14), was extended to describe the ANC time course in breast cancer patients receiving HDC and PBSC transplantation with hematopoietic growth factors support (Fig. 2). The backbone structure of the model consists in five compartments: one compartment represents the proliferative cells [*Prol*], such as stem cell and other progenitor cells; three transit compartments with maturating cells [*Transit*], and one compartment of the circulating blood cells [*Circ*]. A maturation chain, with transit compartments and first-order rate constants (k_{tr}) accounts for the lag time between the HDC administration and the observed neutropenic effects. The generation of new cells in [*Prol*] was dependent on the number of cells in that compartment, which is consistent with the mechanism of self-renewal or mitosis. Therefore, the first-order proliferation rate constant, k_{prol}, determines the rate of cell division, together with the feedback mechanism from the

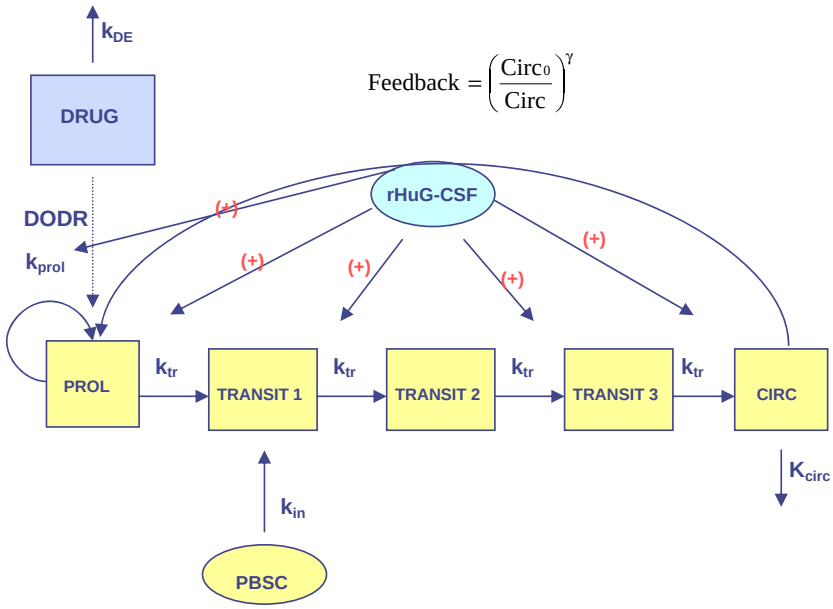

Fig. 2. Schematic of the semi-mechanistic model used to describe the time course of ANC after HDC with PBSC transplantation and hematopoietic growth factors in high risk breast cancer patient.

circulating cells. The feedback loop was necessary to describe the rebound of ANC compared to the baseline values ($Circ_0$) and was incorporated into the model as $(Circ_0/Circ)^{\gamma}$ as previously suggested (14). The feedback function is governed by the γ parameter, which reflects the increase in self-replication rate occurring when circulating cells are depleted.

An additional compartment, [*PBSC*], was needed to account for the effect of the PBSC transplantation on the ANC time course. The amount of PBSC, quantified as the number of CD34+ cells, was assumed to be directly administered on [*PBSC*] at Day 0. The cells in [*PBSC*] were transferred into the first transit compartment following a first-order process determined by $k_{in.}$ Additionally, the effect of transferring the cells in [*PBSC*] to other transit compartments and the zero-order kinetics for that process were also explored. The differential equations describing the reference model were as follows:

$$\frac{dProl}{dt} = k_{\mathrm{Pr}\,ol} \cdot Prol \cdot \left(\frac{Circ_0}{Circ}\right)^{\gamma} \cdot \left(1 - E_{Drug}\right) - k_{tr} \cdot Prol \quad (1)$$

$$\frac{dTransit_1}{dt} = k_{tr} \cdot Prol - k_{tr} \cdot Transit_1 + k_{in} \cdot PBSC \quad (2)$$

$$\frac{dTransit_2}{dt} = k_{tr} \cdot Transit_1 - k_{tr} \cdot Transit_2 \quad (3)$$

$$\frac{dTransit_3}{dt} = k_{tr} \cdot Transit_2 - k_{tr} \cdot Transit_3 \quad (4)$$

$$\frac{dCirc}{dt} = k_{tr} \cdot Transit_3 - k_{Circ} \cdot Circ \quad (5)$$

$$\frac{dPBSC}{dt} = -k_{in} \cdot PBSC \quad (6)$$

The only loss of cells in the transit compartments is into the next compartments and, therefore, the random loss of precursor cells was assumed to be negligible. As the proliferative cells differentiate into more mature cell types, the concentration of cells is maintained by cell division. At steady-state, before administering HDC, *dProl/dt* is equal to 0 and, therefore, k_{Prol}=k_{tr}. As the daily ANC collected did not contain enough information to estimate independently k_{Circ} and k_{tr}, k_{Circ} was fixed to be the population mean half life of neutophils, 0.07 h^{-1} (7). To improve the interpretability, the mean transit time (*MTT*) was estimated as follows:

$$MTT = \frac{n+1}{k_{tr}} \quad (7)$$

where n is the number of transit compartments.

In absence of pharmacokinetic data, a 'kinetics of drug action' model (22), was used to characterize the HDC effect on the inhibition of the proliferation rate and/or stimulation of the killing rate of the progenitor cells according to a linear function:

$$E_{Drug} = \alpha \cdot DODR \quad (8)$$

where *DODR* is a virtual dose-driving rate and α represent the slope that relates the dose-driving rate and the drug effect, E_{Drug}. As STAMP-V regimen is a combination of drugs administered as 96-h infusion, arbitrarily an unitary input rate (U) over 96-h was assumed and the differential equation for this compartment was defined as follows:

$$\frac{dA}{dt} = -k_{DE} \cdot A \quad (9)$$

where, k_{DE} is the first-order equilibration rate of the virtual compartment, which is analogous to the k_{e0} in the effect-compartment model (50); A is the amount in the virtual compartment. Consequently, *DODR* is defined as k_{DE}·A.

According to rHuG-CSF mechanism of action, the influence of rHuG-CSF was incorporated into the model as shortening the *MTT* and increasing the mitotic activity, k_{Prol}. In absence of rHuG-CSF, a dichotomous dummy variable was assigned to have the value 0, whereas in presence of rHuG-CSF the value assigned was one. Therefore, rHuG-CSF effect was incorporated into the model as follows:

$$P^{*} = P_0 \cdot \left(1 + \theta_p \cdot rHuG - CSF\right) \quad (10)$$

where P^{*} is a typical value of the model parameter, which corresponds with P_0 or $P_0 \cdot (1+\theta_P)$ in absence or presence of rHuG-CSF, respectively; and θ_P quantifies the relative contribution of rHuG-CSF effect on the model parameter, P_0. Thus, the system-related model parameters to be estimated were: $Circ_0$, *MTT*, γ, and k_{in}, and the drug-specific parameter to be estimated were: k_{DE}, α and θ_P.

The between subjects variability (BSV) in the model parameters was assumed to follow the lognormal distribution. Residual variability was evaluated using an additive error model after natural logarithmic transformation of the measured ANC and model predictions. The shrinkage for the EBE of the interindividual random effects and residual variability were calculated as previously suggested (24).

Once the reference model was identified and in absence of significant shrinkage, Empirical Bayes Estimates (EBE) of the interindividual random effects were computed and used to identify potential correlation with patient's covariates. Body weight, age, serum creatinine, alkalyne phosphatase, serum alanine aminotransferase (ALT), serum aspartate aminotransferase (AST), serum lactate dehydrogenase (LDH), total bilirubin, total proteins and the amount of PBSC were explored as potential covariates of model parameters following the forward-inclusion and backward-elimination process as described elsewhere (31). These continuous covariates were evaluated using power equations after centering on the median.

Model Selection Criteria

The improvement in the fit obtained for each model was assessed in several ways. First, the resulting NONMEM-generated minimum value of the objective function (MVOF) was used to perform the likelihood ratio test (LRT). This test is based on the change in the MVOF (ΔMVOF), which is equal (up to a constant) to minus twice the log-likelihood of the data and is asymptotically distributed like χ^2 with the degrees of freedom equal to the number of parameters added to the model. ΔMVOFs of −10.83 or −12.12 were required to reach statistical significance at $p \leq 0.0010$ or $p \leq 0.0005$ for the

inclusion or exclusion of one fixed effect, respectively. These stringent statistical criteria were used to avoid the inclusion of weak and clinically no relevant effects. In addition, the improvement in the fit was assessed by the reduction in the BSV and residual variability, the precision in parameter estimates, and the examination of diagnostic plots.

Model Qualification

A non-parametric bootstrap was used as internal evaluation method to qualify the estimates of the model parameters (12) using WINGS for NONMEM (N. Holford, Version 404, June 2003, Auckland, New Zealand). The mean and the 95% confidence intervals of the parameter estimates from the bootstrap replicates were compared with the estimated parameters from the original dataset. In addition, a visual predictive check (VPC) was performed on the time course of ANC. Numerical predictive checks (NPC) were conducted to evaluate the model predictive performance on the mean of the ANC at nadir, the mean time to reach the ANC nadir, and mean time to recover from Grade 4 neutropenia.

RESULTS

The model proposed by Friberg *et al.* provided a reasonable fit to the data with slight ANC under prediction after the recovery of Grade 4 neutropenia, probably because the effects of PBSC and rHuG-CSF were not accounted for. Actually, a reduction in the MVOF of 212.93, 223.91, 236.56, 242.66 or 167.19 units was achieved by adding the [*PBSC*] into the model and linking it to [*Circ*], [$Transit_3$], [$Transit_2$], [$Transit_1$] or [*Prol*], respectively, through a first-order rate constant. Based on these results, the [*PBSC*] was linked to [$Transit_1$], however further improvement was obtained when the zero-order, instead of first-order, process was employed (ΔMVOF = −50.99). The fact that cells in [*PBSC*] entered into [$Transit_1$] assume that the transplanted cells will mature into the neutrophils, but will not be proliferating. This assumption allowed a better description of the data than if cells in [*PBSC*] would have entered into [*Prol*], which implies that the transplanted cells will proliferate and then mature to become neutrophils.

The rHuG-CSF effect was evaluated as time-dependent dichotomous variable for the *MTT*, k_{prol} and γ, separately. The univariate analysis indicated a statistically significant effect of rHuG-CSF on *MTT* (ΔMVOF=−15.94, d.f.=1, $p<0.001$), k_{prol} (ΔMVOF=−13.99, d.f.=1, $p<0.001$) and γ (ΔMVOF=−13.99, d.f.=1, $p<0.001$). The rHuG-CSF effect on *MTT* and k_{prol} was incorporated simultaneously in the model (ΔMVOF=−44.69, d.f.=2, $p<0.001$) and the sequential inclusion of the rHuG-CSF effect on γ did not result in further improvement of the fit.

A linear function of the *DODR* was useful in describing the HDC effect on the inhibition of the proliferation rate and/or stimulation of the killing rate of the progenitor cells. Attempts to characterize the E_{Drug} as an E_{max} or log-linear model failed as the parameters could not be reliably estimated, probably because all patients received the same dosing schedule.

The BSV of $Circ_0$, *MTT*, k_{in}, k_{DE} and α were estimated with reasonably precision (<53%) and the associated shrinkage was estimated to be 0.212, 0.131, 0.077, 0.128 and 0.108, respectively. Attempts to estimate the BSV on γ failed,

Table II. Parameter Estimates and Bootstrap Analysis of the Final Model

Model parameters	Original dataset	Non-Parametric bootstrap	
	Parameter estimate[a] (RSE)	Mean[a] (RSE)	95%Confidence interval
System-related parameter			
$Circ_0$ ($\cdot 10^6$/L)	5,610 (4.62)	5,620 (4.71)	5,110–6,150
MTT (h)	92.3 (25.7)	95.7 (30.8)	52.6–175
γ	0.145 (13.3)	0.143 (16.4)	0.097–0.18
k_{in} ($\cdot 10^6$cell/kg/day)	0.954 (9.97)	0.938 (14.0)	0.75–1.15
Drug-related parameter			
k_{DE} ($\cdot 10^{-3}$h^{-1})	7.11 (7.86)	7.28 (10.3)	6.13–8.82
α	2.50 (3.75)	2.49 (5.15)	2.21–2.69
rHuG-CSF Effect (%)			
-Reduction of MTT	48.0 (25.7)	49.5 (30.8)	36.6–62.5
-Increase of k_{prol}	120 (25.3)	127 (30.0)	72.7–213
Covariates effects			
PBSC covariate on γ	0.15 (45.5)	0.15 (56.9)	0.013–0.34
Interindividual Variability[b]			
$\omega(Circ_0)$	19.2 (41.9)	18.9 (50.7)	9.48–27.5
$\omega(MTT)$	14.0 (37.0)	13.9 (39.5)	8.01–27.5
$\omega(k_{in})$ [c]	44.9 (30.1)	45.7 (33.8)	32.8–63.0
$\omega(k_{DE})$	41.0 (29.9)	40.7 (30.9)	28.2–51.3
$\omega(\alpha)$[c]	11.3 (52.8)	11.3 (54.6)	5.71–16.3
Residual Variability (%)	45.30 (4.76)	44.9 (4.74)	41.0–48.8

[a] Results expressed as parameter (RSE: relative standard error of the parameter estimate, %)
[b] Results expressed as coefficient of variation, %. (RSE: relative standard error of the ω^2, %)
[c] Correlation between IIV of k_{in} and α is−0.62, 95%CI (−0.91,−0.40)

probably because the data available did not support its estimation. In addition, the magnitude of the residual variability was estimated to be similar to the values previously reported and the associated shrinkage was estimated to be relatively low, 0.0785. Taken together these results enable the use of Empirical Bayesian Estimates of model parameters to explore potential correlations with patient's covariates. In the screening analysis, no covariates were found to have statistically significant correlation with the model parameters, except the PBSC effect on γ (ΔMVOF=−12.85, d.f.=1, $p<$ 0.001) which was incorporated into the model. Furthermore, the correlation between α and k_{in} was found to be relevant and, consequently, the off-diagonal element of the variance-covariance matrix was added into the model.

The final estimates of model parameters and the results of the non-parametric bootstrap are presented in Table II. Diagnostic plots displayed in Fig. 3 showed tight random normal scatter around the identity line, indicating an absence of bias and confirming the adequacy of the model to describe the data, while histograms of random effects exhibited normal distribution (data not shown). From 1,000 replicates analyzed during the bootstrap analysis, 32.5% failed to minimize

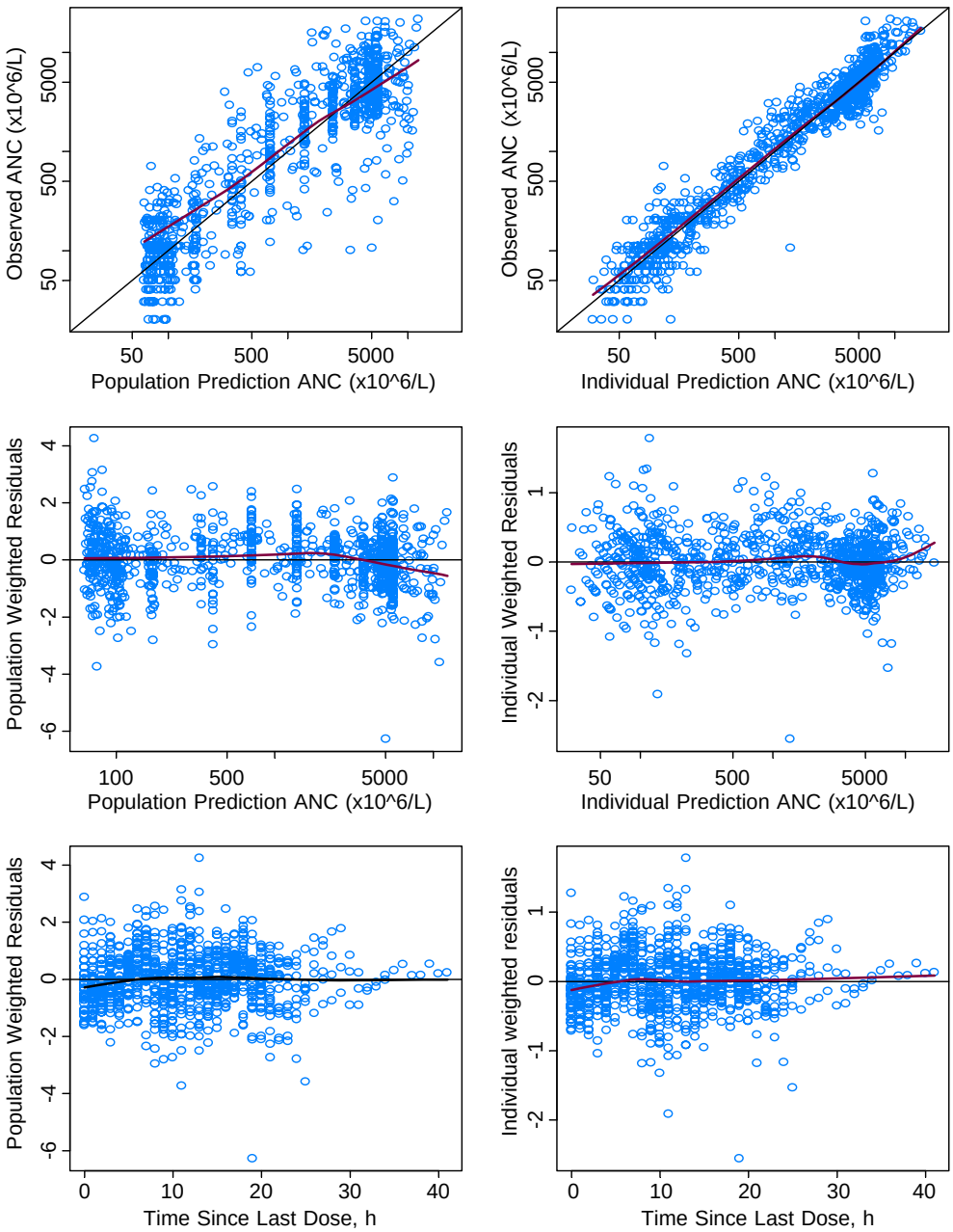

Fig. 3. Diagnostic plots for the final model. *Upper panels* show absolute neutrophil counts *versus* population (*left*) and individual (*right*) model predictions. *Mid panels* show the weighted residuals *versus* population (*left*) and individual (*right*) model predictions. *Lower panels* show the population (*left*) and individual (*right*) weighted residuals *versus* time. The *black thin line* represents the identity line and the *red bold line* represents the smoother line.

successfully and were excluded. The population estimates for the final model were similar to the mean of the non-parametric bootstrap replicates that minimized successfully and were contained within the 95% confidence intervals. The precision of the NONMEM parameter estimates was also acceptable as the relative standard error (RSE) presented in Table II were lower than 53%. These findings suggested a high accuracy and precision of the NONMEM parameter estimates.

The results of the VPC on the ANC time course displayed in Fig. 4 further confirmed the adequacy of the model to describe the data. Actually, 91.35% and 95.35% of the observed data fall inside the 90% and 95% prediction intervals, respectively. Figure 5 displays the NPC performed on the ANC nadir, time to ANC nadir and time to recover from the Grade 4 neutropenia. These results evidence the validity of the model to predict clinically relevant outcomes as a function of the beginning of rHuG-CSF treatment and the amount of CD34+ cells infused. The mean ANC nadir ranged from 40 to $110 \cdot 10^6$/L and the mean time to nadir ranged from 11 to 14 days from the start of chemotheraphy, and both were independent of the beginning of rHuG-CSF treatment or the amount of PBSC cells infused. Interestingly, there was a trend to have shorter neutropenia recovery when rHuG-CSF was initiated on Day +1 and the amount of PBSC was greater than $5 \cdot 10^6$/Kg. In this situation, the model predicted mean time to recovery from the Grade 4 neutropenia was 8.6 days (95%CI: 7.6–9.6 days), which is about 2 days shorter than the estimated value of 10.5 days (95%CI: 9.6–11.5 days) when rHuG-CSF was initiated on Day +5 and the amount of CD34+ cells is lower than $5 \cdot 10^6$/Kg.

DISCUSSION

The model described by Friberg *et al.* (14) has been successfully used to characterize the neutropenia induced by several anticancer drugs. However, it has not been applied before to analyze the data obtained from patients undergoing HDC, which usually produces a severe Grade 4 neutropenia in the vast majority of the patients. In this paper, an extension of that model has been developed in absence of pharmacokinetic data and, after accounting for the effects of PBSC and rHuG-CSF support, has been successfully applied to characterize the time course of ANC after the administration of STAMP-V chemotherapy to high-risk breast cancer.

Several authors have suggested methods for analyzing dose-response time data in absence of pharmacokinetic data (15). In addition, sometimes may be convenient or necessary to simplify the pharmacokinetic information and use alternative approaches such as the 'kinetics of drug action' concept (K-PD model) previously introduced (22). In this study the absence of the pharmacokinetic data of cyclophosphamide,

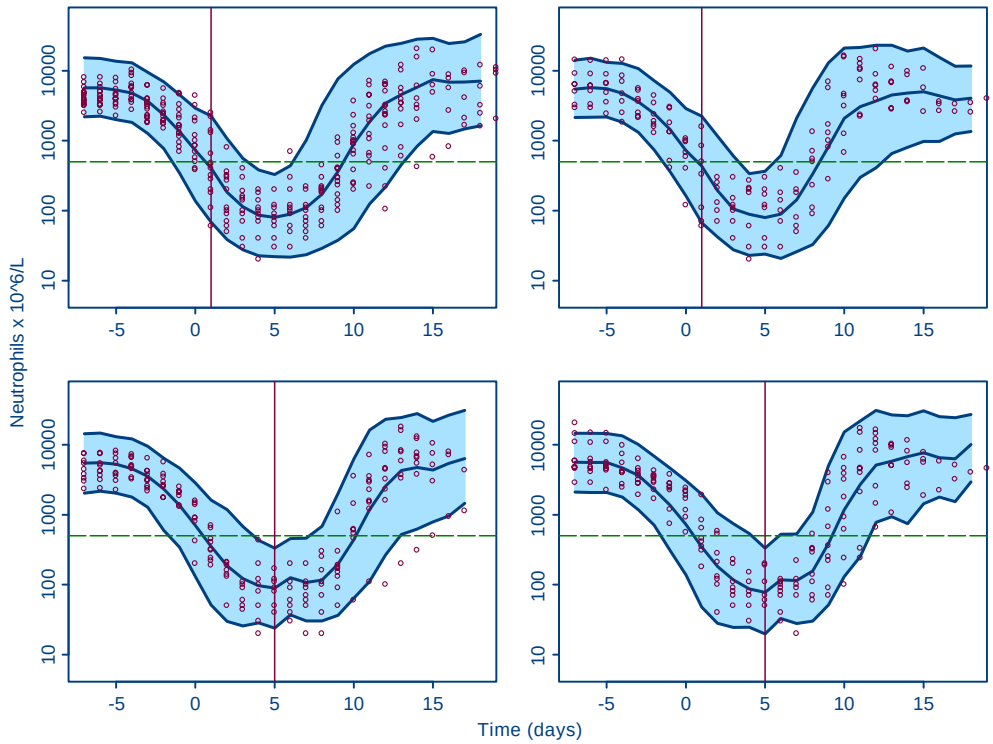

Fig. 4. Visual predictive check for the time course of ANC stratified by the amount of CD34+ cells transplanted and the beginning of rHuG-CSF treatment. *Left panels* represent the visual predictive check for subjects who received CD34+ cells equal or lower than $5 \cdot 10^6$ cells/kg, while the *right panel* represents the visual predictive check for subjects who received CD34+ cells greater than $5 \cdot 10^6$ cells/kg. *Upper panels* represent subjects who had the beginning of rHuG-CSF treatment on Day +1 (*upper panels*) or Day +5 (*lower panels*). *Solid blue line* represents the 5th, 50th, and 95th percentiles of the simulated ANC, the *shaded area* represents the 90% prediction interval, *vertical red line* represents the beginning of rHuG-CSF treatment and the *dashed green horizontal line* represents the absolute neutrophils counts of $500 \cdot 10^6$/L, representative of Grade 4 neutropenia.

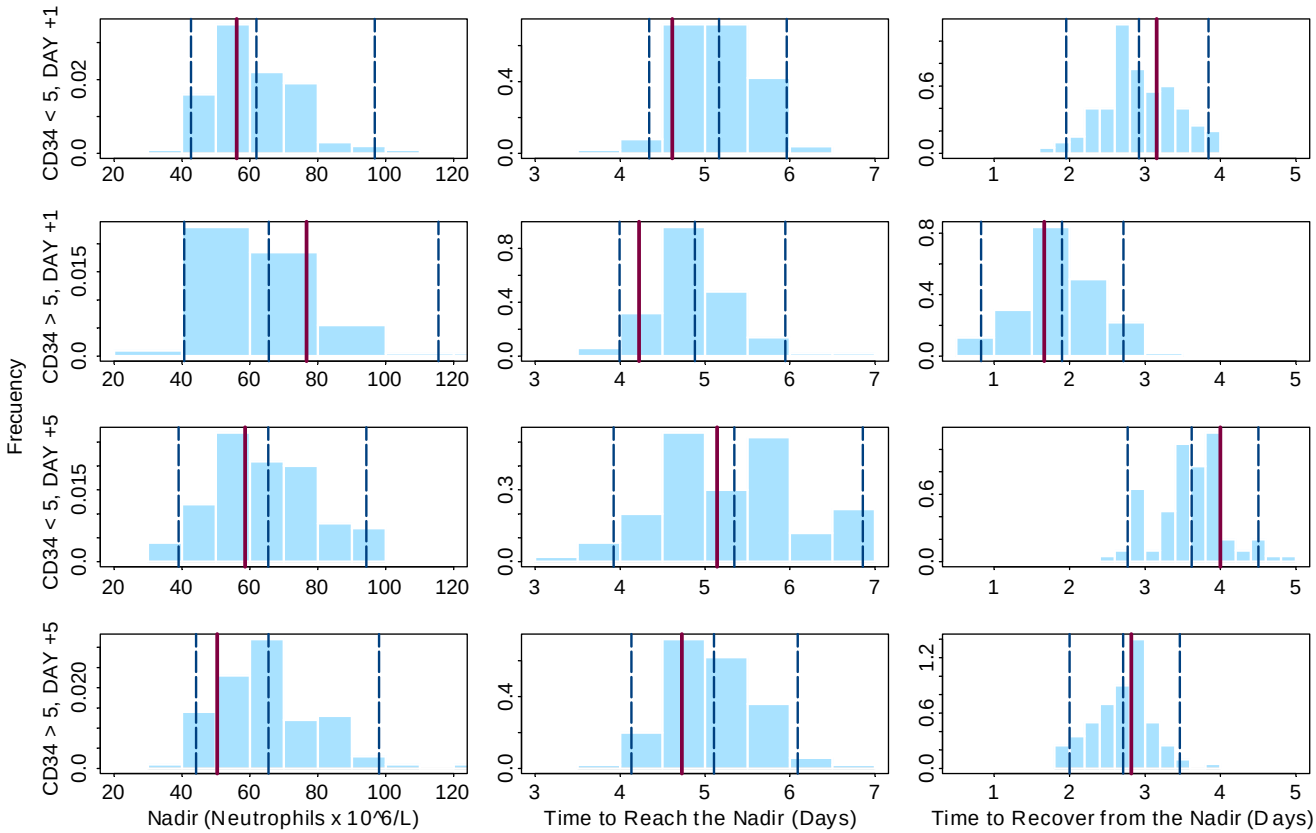

Fig. 5. Predictive check for the mean nadir of ANC (*left panels*), mean time to reach the nadir (*mid panels*) and mean time to recover from the nadir (*right panels*), stratified by the amount of CD34+ cells transplanted and the beginning of rHuG-CSF treatment. *Vertical dashed blue lines* represent the 5th, 50th, and 95th percentiles of the simulated distribution of the mean parameter and *vertical red line* represent the observed mean parameter.

thiotepa and carboplatin has determinated the use of the K-PD approach. An alternative approach could be to assume for all patients the typical time course of cyclophosphamide, thiotepa and carboplatin plasma concentrations based on a published model (8), and try to estimate the relative contribution of each compound on the neutropenic effect. However, such an approach has two main limitations. First, there is no data available quantifying the neutropenic effects of monotherapy with each drug used in the STAMP-V protocol, thus, the relative effect of the combination of the three compounds could not be uniquely identified. On the other hand, cyclophosphamide, thiotepa and carboplatin were administered as 96-h continuous infusion in the STAMP-V protocol, while data from intermittent daily infusions for 4 days were used to develop the published model (8). Considering the interplay of the cyclophosphamide, thiotepa and carboplatin pharmacokinetics when administered concomitantly, the lack of model validation for continuous infusion administration and the difficulty in estimating the relative contribution of each drug to the neutropenic effect, the K-PD approach was used. This approach have been successfully used before to characterize rich pharmacody-

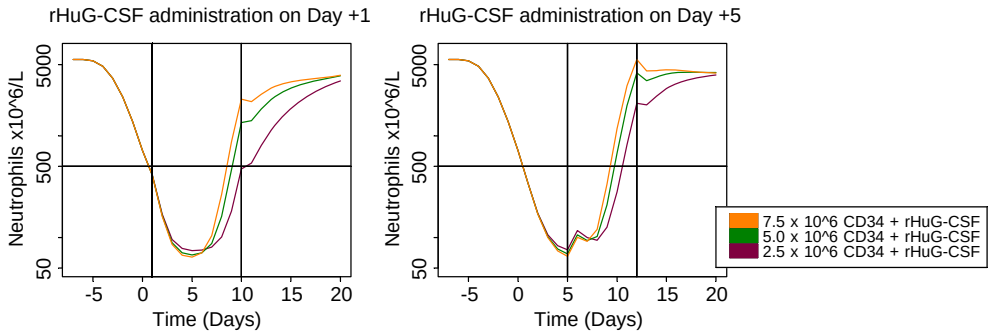

Fig. 6. Deterministic simulations showing the effect of the amount of CD34+ cells transplanted. Vertical lines represent the beginning and end of rHuG-CSF treatment and horizontal line represents the absolute neutrophils counts of 500·106/L, representative of Grade 4 neutropenia.

namic profiles such as the effect of morphine on hypoxic and hypercapnic breathing (42) and the effect of ibandronate on the osteoclast activity monitored by the urinary CTx (40).

Nevertheless, the complexity of the present model was limited because it was developed from only one type of observation, such as ANC, and no data on precursor cells were available. However, with relatively few parameters, the model incorporates many important structural features of the hematopoietic system, such as cell production, maturation and degradation as well as the effect of PBSC and rHuG-CSF.

The HDC effect on the inhibition of the proliferation rate and/or the stimulation of the killing rate of the progenitor cells was modelled according to a linear function of the *DODR*. According to Eq. 8, when E_{Drug} function is equal to 1, the inhibition of the cell proliferative rate into [*Prol*] was completed, which happened in about 50% of the patients approximately three days after the treatment started and, it lasted for 1 day after the chemotherapy ends. During that period of time, the HDC also stimulate the killing rate of the progenitor cells.

A [*PBSC*] compartment was linked to [$Transit_1$], which is consistent with nature of stems cells and its physiology, where k_{in} accounts for the PBSC effect on the neutropenia recovery as evidenced in the deterministic simulations presented in Fig. 6. Consistent with the estimated value of k_{in}, $0.954 \cdot 10^6$cell/kg/day, and the data previously published (51), the time to recovery from neutropenia Grade 4 decrease as the amount of CD34+ cells infused increased, independently of the beginning of the rHu-G-CSF support.

In our model, the influence of rHuG-CSF was incorporated as shortening the *MTT* and increasing the mitotic activity as described in previous papers (45), however this implementation is no accounting for the pharmacokinetic and pharmacodynamic complexities of rHuG-CSF recently published in healthy subjects (44). Nevertheless, it is well known rHuG-CSF decreases maturation times for postmitotic cells and stimulates mitosis and mobilization of band cells and segmented neutrophils in bone marrow (33,41,56), which, therapeutically, translates in shortening the duration of neutropenia Grade 4 (9). Actually, rHuG-CSF decreased the *MTT* by 92%, while increased the mitotic activity by 120%, which is consistent with the reported values presented recently (36,45) and the slight trend evidenced in the deterministic simulations (Fig. 6) to reduce the time to recovery from severe neutropenia for the earlier administration of the rHuG-CSF. Notably, these effects were independent of the amount of CD34+ cells infused.

Despite differing from the Friberg's model in a number of ways, the modified model shares a number of common features. Actually, the estimates of the typical values of the system-related parameters, $Circ_0$, *MTT* and γ, were similar to those obtained previously (14,21,23,26–30,36,45,46,55,57), including *MTT*, which was estimated at the lower end of the values found in other studies (14,26). In addition, the graphical exploratory analysis of the effect of body weight, age, serum creatinine, alkalyne phosphatase, ALT, AST, LDH, total bilirubin and total proteins on the model parameter did not evidence any statistical significant correlation, which is consistent with the results of a recent publication where these covariates were not statistically associated or had no clinically relevant effect on the model parameters derived for docetaxel, paclitaxel etoposide and topotecan (27). Only the effect of PBSC on γ from Day 0 onwards was incorporated in the model, although the magnitude of the effect probably is not clinically relevant as doubling the amount of CD34+ cells infused resulted in only 11% increase in γ. Interindividual and residual variabilities were moderate to large, consistently with what has been observed for other drugs (14).

Non-parametric bootstrap, VPC and NPC were used as complementary methods to assess the validity of the model for predictive purposes. The results of the non-parametric bootstrap analysis confirmed the accuracy and precision in the estimates of model parameters, while the NPC evidenced the adequacy of the model to predict the time course of ANC, including the ANC nadir, the time to ANC nadir and the time to recover from Grade 4 neutropenia. As a result, the successful qualification of the model provides supportive evidence that the severity and the duration of neutropenia can be predicted in high-risk breast cancer patients receiving HDC with PBSC and rHuG-CSF support. Consequently, model-based simulation can be undertaken to explore the optimal timing to initiate the treatment with rHuG-CSF and the amount of PBSC needed to have the shorter time to recover from severe neutropenia.

The data used in the current analysis were obtained after the single administration of the STAMP-V protocol in high-risk breast cancer patients without any pharmacokinetic data and, consequently, the model parameters, specially the drug-specific parameters, should be cautiously considered if model simulations are intended to infer the outcomes for other doses, schedules, combinations of drugs, patient population or multiple course of the STAMP-V regimen, for which the model has not been qualified. Therefore, the model needs to be updated as more information becomes available from other studies under different dosing scenarios or other patient population.

In summary, the semi-mechanistic model developed by Friberg *et al.* has been expanded to account for the PBSC transplantation and rHuG-CSF support, in absence of pharmacokinetic information. The modified model has been successfully applied to describe the time course of ANC in high-risk breast cancer patients receiving HDC and no patient specific covariates were found to be statistically associated with model parameters. In addition, the higher amount of CD34+ cells together with the earlier administration rHuG-CSF was associated with faster haematological recovery.

ACKNOWLEDGEMENTS

The authors would like to thank the patients, investigators (Dra. Ana Lluch and Dr. Daniel Almenar) and their medical, nursing and laboratory staff who participated in the study. In addition, the authors recognize the valuable comments provided by Dr. N. Victor Jimenez and Dr. Vicente G. Casabó at the beginning of the analysis.

Conflict of Interest This study was supported by Grant 97/0758 from Fondo de Investigaciones Sanitarias, Ministerio de Sanidad (Spain). The authors disclosure none conflict of interest other than Juan Jose Perez Ruixo is AMGEN employee since May 2007.

REFERENCES

1. Antman K, Ayash L, Elias A, Wheeler C, Hunt M, Eder JP, *et al*. A phase II study of high-dose cyclophosphamide, thiotepa, and carboplatin with autologous marrow support in women with measurable advanced breast cancer responding to standard-dose therapy. J Clin Oncol. 1992;10:102–10.
2. Armitage JO. Bone marrow transplantation. N Engl J Med. 1994;330:827–38. doi:10.1056/NEJM199403243301206.
3. Attal M, Harousseau JL, Stoppa AM, Sotto JJ, Fuzibet JG, Rossi JF, *et al*. A prospective, randomized trial of autologous bone marrow transplantation and chemotherapy in multiple myeloma. Intergroupe Francais du Myelome. N Engl J Med. 1996;335:91–7. doi:10.1056/NEJM199607113350204.
4. Attal M, Huguet F, Schlaifer D, Payen C, Laroche M, Fournie B, *et al*. Intensive combined therapy for previously untreated aggressive myeloma. Blood. 1992;79:1130–6.
5. Beal SL, Sheiner LB. NONMEM users guides. Hanover (MD): GloboMax, LLC.; 1992.
6. Beyer J, Schwella N, Zingsem J, Strohscheer I, Schwaner I, Oettle H, *et al*. Hematopoietic rescue after high-dose chemotherapy using autologous peripheral-blood progenitor cells or bone marrow: a randomized comparison. J Clin Oncol. 1995; 13:1328–35.
7. Dale DC, Liles WC, Llewellyn C, Price TH. Effects of granulocyte-macrophage colony-stimulating factor (GM-CSF) on neutrophil kinetics and function in normal human volunteers. Am J Hematol. 1998;57:7–15. doi:10.1002/(SICI)1096-8652(199801)57:1<7::AID-AJH2>3.0.CO;2-0.
8. de Jonge ME, Huitema AD, Rodenhuis S, Beijnen JH. Integrated population pharmacokinetic model of both cyclophosphamide and thiotepa suggesting a mutual drug-drug interaction. J Pharmacokinet Pharmacodyn. 2004;31:135–56. doi:10.1023/B:JOPA.0000034405. 03895.c2.
9. Dekker A, Bulley S, Beyene J, Dupuis LL, Doyle JJ, Sung L. Meta-analysis of randomized controlled trials of prophylactic granulocyte colony-stimulating factor and granulocyte-macrophage colony-stimulating factor after autologous and allogeneic stem cell transplantation. J Clin Oncol. 2006;24:5207–15. doi:10.1200/JCO.2006.06.1663.
10. Dillman RO, Barth NM, Nayak SK, DeLeon C, O'Connor A, Morrelli L. High-dose chemotherapy with autologous stem cell rescue in breast cancer. Breast Cancer Res Treat. 1996;37:277–89. doi:10.1007/BF01806509.
11. Elias AD, Ayash L, Anderson KC, Hunt M, Wheeler C, Schwartz G, *et al*. Mobilization of peripheral blood progenitor cells by chemotherapy and granulocyte-macrophage colony-stimulating factor for hematologic support after high-dose intensification for breast cancer. Blood. 1992;79:3036–44.
12. Ette EI. Stability and performance of a population pharmacokinetic model. J Clin Pharmacol. 1997;37:486–95.
13. Ferreri AJ, Crocchiolo R, Assanelli A, Govi S, Reni M. High-dose chemotherapy supported by autologous stem cell transplantation in patients with primary central nervous system lymphoma: facts and opinions. Leuk Lymphoma. 2008;49:2042–7. doi:10.1080/10428190802381238.
14. Friberg LE, Henningsson A, Maas H, Nguyen L, Karlsson MO. Model of chemotherapy-induced myelosuppression with parameter consistency across drugs. J Clin Oncol. 2002;20:4713–21. doi:10.1200/JCO.2002.02.140.
15. Gabrielsson J, Jusko WJ, Alari L. Modeling of dose-response-time data: four examples of estimating the turnover parameters and generating kinetic functions from response profiles. Biopharm Drug Dispos. 2000;21:41–52. doi:10.1002/1099-081X(200003) 21:2<41::AID-BDD217>3.0.CO;2-D.
16. Gill P, Litzow M, Buckner J, Arndt C, Moynihan T, Christianson T, *et al*. High-dose chemotherapy with autologous stem cell transplantation in adults with recurrent embryonal tumors of the central nervous system. Cancer. 2008;112:1805–11. doi:10.1002/cncr.23362.
17. Greb A, Bohlius J, Schiefer D, Schwarzer G, Schulz H, Engert A. 2008. High-dose chemotherapy with autologous stem cell transplantation in the first line treatment of aggressive non-Hodgkin lymphoma (NHL) in adults. Cochrane Database Syst Rev. CD004024
18. Gianni AM, Siena S, Bregni M, Tarella C, Stern AC, Pileri A, *et al*. Granulocyte-macrophage colony-stimulating factor to harvest circulating haemopoietic stem cells for autotransplantation. Lancet. 1989;2:580–5. doi:10.1016/S0140-6736(89) 90711-3.
19. Grigg A, Begley CG, Juttner CA, Szer J, To LB, Maher D, *et al*. Effect of peripheral blood progenitor cells mobilised by filgrastim (G-CSF) on platelet recovery after high-dose chemotherapy. Bone Marrow Transplant. 1993;11(Suppl 2):23–9.
20. Hillner BE, Smith TJ, Desch CE. Cost-effective use of autologous bone marrow transplantation: few answers, many questions, and suggestions for future assessments. Pharmacoeconomics. 1994;6:114–26. doi:10.2165/00019053-199406020-00004.
21. Hing J, Perez-Ruixo JJ, Stuyckens K, Soto-Matos A, Lopez-Lazaro L, Zannikos P. Mechanism-based pharmacokinetic/pharmacodynamic meta-analysis of trabectedin (ET-743, Yondelis®) induced neutropenia. Clin Pharmacol Ther. 2008;83:130–43. doi:10.1038/sj.clpt.6100259.
22. Jacqmin P, Snoeck E, van Schaick EA, Gieschke R, Pillai P, Steimer JL, *et al*. Modelling response time profiles in the absence of drug concentrations: definition and performance evaluation of the K-PD model. J Pharmacokinet Pharmacodyn. 2007;34:57–85. doi:10.1007/s10928-006-9035-z.
23. Joerger M, Huitema AD, Richel DJ, Dittrich C, Pavlidis N, Briasoulis E, *et al*. Population pharmacokinetics and pharmacodynamics of paclitaxel and carboplatin in ovarian cancer patients: a study by the European organization for research and treatment of cancer-pharmacology and molecular mechanisms group and new drug de. Clin Cancer Res. 2007;13:6410–8. doi:10.1158/1078-0432.CCR-07-0064.
24. Karlsson MO, Savic RM. Diagnosing model diagnostics. Clin Pharmacol Ther. 2007;82:17–20. doi:10.1038/sj.clpt.6100241.
25. Karlsson MO, Anehall T, Friberg LE, Henningsson A, Kloft C, Sandström M, *et al*. Pharmacokinetic/pharmacodynamic modelling in oncological drug development. Basic Clin Pharmacol Toxicol. 2005;96:206–11. doi:10.1111/j.1742-7843.2005.pto960310.x.
26. Kathman SJ, Williams DH, Hodge JP, Dar M. A Bayesian population PK-PD model of ispinesib-induced myelosuppression. Clin Pharmacol Ther. 2007;81:88–94. doi:10.1038/sj.clpt.6100021.
27. Kloft C, Wallin J, Henningsson A, Chatelut E, Karlsson MO. Population pharmacokinetic-pharmacodynamic model for neutropenia with patient subgroup identification: comparison across anticancer drugs. Clin Cancer Res. 2006;12:5481–90. doi:10.1158/1078-0432.CCR-06-0815.
28. Latz JE, Karlsson MO, Rusthoven JJ, Ghosh A, Johnson RD. A semimechanistic-physiologic population pharmacokinetic/pharmacodynamic model for neutropenia following pemetrexed therapy. Cancer Chemother Pharmacol. 2005;57:412–26. doi:10.1007/s00280-005-0077-5.
29. Latz JE, Rusthoven JJ, Karlsson MO, Ghosh A, Johnson RD. Clinical application of a semimechanistic-physiologic population PK/PD model for neutropenia following pemetrexed therapy. Cancer Chemother Pharmacol. 2005;57:427–35. doi:10.1007/s00280-005-0035-2.
30. Leger F, Loos WJ, Bugat R, Mathijssen RH, Goffinet M, Verweij J, *et al*. Mechanism-based models for topotecan-induced neutropenia. Clin Pharmacol Ther. 2004;76:567–78. doi:10.1016/j.clpt.2004.08.008.
31. Mandema JW, Verotta D, Sheiner LB. Building population pharmacokinetic-pharmacodynamic models. I. Models for covariate effects. J Pharmacokinet Biopharm. 1992;20:511–28. doi:10.1007/BF01061469.
32. Minami H, Sasaki Y, Saijo N, Ohtsu T, Fujii H, Igarashi T, *et al*. Indirect-response model for the time course of leukopenia with anticancer drugs. Clin Pharmacol Ther. 1998;64:511–21. doi:10.1016/S0009-9236(98) 90134-5.
33. Mukae H, Zamfir D, English D, Hogg JC, van Eeden SF. Polymorphonuclear leukocytes released from the bone marrow by granulocyte colony-stimulating factor: intravascular behavior. Hematol J. 2000;1:159–71. doi:10.1038/sj.thj.6200023.
34. Muramatsu T, Shinozuka T, Hirasawa T, Tsukada H, Maeda H, Miyamoto T, *et al*. Treatment strategy for recurrent and refractory epithelial ovarian cancer: efficacy of high-dose chemotherapy with hematopoietic stem cell transplantation. Acta Histochem Cytochem. 2006;39:61–7. doi:10.1267/ahc.05030.

35. Nitz UA, Mohrmann S, Fischer J, Lindemann W, Berdel WE, Jackisch C, *et al*. Comparison of rapidly cycled tandem high-dose chemotherapy plus peripheral-blood stem-cell support *versus* dose-dense conventional chemotherapy for adjuvant treatment of high-risk breast cancer: results of a multicentre phase III trial. Lancet. 2005;366:1935–44. doi:10.1016/S0140-6736(05) 67784-7.
36. Panetta JC, Schaiquevich P, Santana VM, Stewart CF. Using pharmacokinetic and pharmacodynamic modeling and simulation to evaluate importance of schedule in topotecan therapy for pediatric neuroblastoma. Clin Cancer Res. 2008;14:318–25. doi:10.1158/1078-0432.CCR-07-1243.
37. Pedrazzoli P, Rosti G, Secondino S, Carminati O, Demirer T. High-dose chemotherapy with autologous hematopoietic stem cell support for solid tumors in adults. Semin Hematol. 2007;44:286–95. doi:10.1053/j.seminhematol.2007.08.009.
38. Peters WP, Ross M, Vredenburgh JJ, Meisenberg B, Marks LB, Winer E, *et al*. High-dose chemotherapy and autologous bone marrow support as consolidation after standard-dose adjuvant therapy for high-risk primary breast cancer. J Clin Oncol. 1993;11:1132–43.
39. Peters WP, Rosner GL, Vredenburgh JJ, Shpall EJ, Crump M, Richardson PG, *et al*. Prospective, randomized comparison of high-dose chemotherapy with stem-cell support *versus* intermediate-dose chemotherapy after surgery and adjuvant chemotherapy in women with high-risk primary breast cancer: a report of CALGB 9082, SWOG 9114, and NCIC MA-13. J Clin Oncol. 2005;23(10):2191–200. doi:10.1200/JCO.2005.10.202.
40. Pillai G, Gieschke R, Goggin T, Jacqmin P, Schimmer RC, Steimer JL. A semimechanistic and mechanistic population PK-PD model for biomarker response to ibandronate, a new bisphosphonate for the treatment of osteoporosis. Br J Clin Pharmacol. 2004;58:618–31. doi:10.1111/j.1365-2125.2004.02224.x.
41. Price TH, Chatta GS, Dale DC. Effect of recombinant granulocyte colony-stimulating factor on neutrophil kinetics in normal young and elderly humans. Blood. 1996;88:335–40.
42. Romberg R, Olofsen E, Sarton E, Teppema L, Dahan A. Pharmacodynamic effect of morphine-6-glucuronide *versus* morphine on hypoxic and hypercapnic breathing in healthy volunteers. Anesthesiology. 2003;99:788–98. doi:10.1097/00000542-200310000-00008.
43. Rombout F, Aarons L, Karlsson M, Man A, Mentré F, Nygren P, *et al*. Modelling and simulation in the development and use of anti-cancer agents: an underused tool? J Pharmacokinet Pharmacodyn. 2004;31:419–40. doi:10.1007/s10928-005-5910-2.
44. Roskos LK, Lum P, Lockbaum P, Schwab G, Yang BB. Pharmacokinetic/pharmacodynamic modeling of pegfilgrastim in healthy subjects. J Clin Pharmacol. 2006;46:747–57. doi:10.1177/0091270006288731.
45. Sandstrom M, Lindman H, Nygren P, Johansson M, Bergh J, Karlsson MO. Population analysis of the pharmacokinetics and the haematological toxicity of the fluorouracil-epirubicin-cyclophosphamide regimen in breast cancer patients. Cancer Chemother Pharmacol. 2006;58:143–56. doi:10.1007/s00280-005-0140-2.
46. Sandstrom M, Lindman H, Nygren P, Lidbrink E, Bergh J, Karlsson MO. Model describing the relationship between pharmacokinetics and hematologic toxicity of the epirubicin-docetaxel regimen in breast cancer patients. J Clin Oncol. 2005;23:413–21. doi:10.1200/JCO.2005.09.161.
47. Schmoor C, Sauerbrei W, Bastert G, Bojar H, Schumacher M, German Breast Cancer Study Group. Long-term prognosis of breast cancer patients with 10 or more positive lymph nodes treated with CMF. Eur J Cancer. 2001;37:1123–31.
48. Schulman KA, Birch R, Zhen B, Pania N, Weaver CH. Effect of CD34(+) cell dose on resource utilization in patients after high-dose chemotherapy with peripheral-blood stem-cell support. J Clin Oncol. 1999;17:1227–33.
49. Schwartzberg L, Birch R, Blanco R, Wittlin F, Muscato J, Tauer K, *et al*. Rapid and sustained hematopoietic reconstitution by peripheral blood stem cell infusion alone following high-dose chemotherapy. Bone Marrow Transplant. 1993;11:369–74.
50. Sheiner LB, Stanski DR, Vozeh S, Miller RD, Ham J. Simultaneous modeling of pharmacokinetics and pharmacodynamics: application to d-tubocurarine. Clin Pharmacol Ther. 1979;25:358–71.
51. Shpall EJ, Champlin R, Glaspy JA. Effect of CD34+ peripheral blood progenitor cell dose on hematopoietic recovery. Biol Blood Marrow Transplant. 1998;4:84–92. doi:10.1053/bbmt.1998.v4.pm9763111.
52. Stadtmauer EA, O'Neill A, Goldstein LJ, Crilley PA, Mangan KF, Ingle JN, *et al*. Conventional-dose chemotherapy compared with high-dose chemotherapy plus autologous hematopoietic stem-cell transplantation for metastatic breast cancer. Philadelphia Bone Marrow Transplant Group. N Engl J Med. 2000;342:1069–76. doi:10.1056/NEJM200004133421501.
53. Testart-Paillet D, Girard P, You B, Freyer G, Pobel C, Tranchand B. Contribution of modelling chemotherapy-induced hematological toxicity for clinical practice. Crit Rev Oncol Hematol. 2007;63:1–11. doi:10.1016/j.critrevonc.2007.01.005.
54. To LB, Dyson PG, Branford AL, Russell JA, Haylock DN, Ho JQ, *et al*. Peripheral blood stem cells collected in very early remission produce rapid and sustained autologous haemopoietic reconstitution in acute non-lymphoblastic leukaemia. Bone Marrow Transplant. 1987;2:103–8.
55. Troconiz IF, Garrido MJ, Segura C, Cendrós JM, Principe P, Peraire C, *et al*. Phase I dose-finding study and a pharmacokinetic/pharmacodynamic analysis of the neutropenic response of intravenous diflomotecan in patients with advanced malignant tumours. Cancer Chemother Pharmacol. 2006;57:727–35. doi:10.1007/s00280-005-0112-6.
56. Ulich TR, del Castillo J, Souza L. Kinetics and mechanisms of recombinant human granulocyte-colony stimulating factor-induced neutrophilia. Am J Pathol. 1988;133:630–8.
57. Van Kesteren KC, Zandvliet AS, Karlsson MO, Mathôt RA, Punt CJ, Armand JP, *et al*. Semi-physiological model describing the hematological toxicity of the anti-cancer agent indisulam. Invest New Drugs. 2005;23:225–34. doi:10.1007/s10637-005-6730-3.
58. Weissbach L, Beyer J. High-dose chemotherapy and hematopoietic stem cell transplantation in patients with germ cell cancer. Urologe A. 2007;46:416–9. doi:10.1007/s00120-007-1318-5.